

# The Effect of Viscoelastic Fluids on Flows Generated by Spherical Objects during Sedimentation

By

Latifah binti Hamzah

Submitted to the Department of Mechanical Engineering  
in Partial Fulfillment of the Requirements for the Degree of

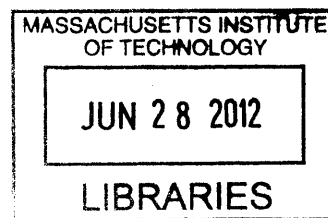
Bachelor of Science in Mechanical Engineering

at the

MASSACHUSETTS INSTITUTE OF TECHNOLOGY

June 2012

**ARCHIVES**



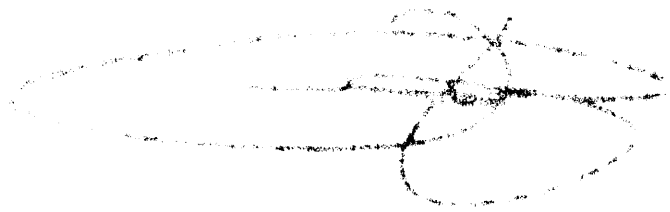
©MMXII Latifah binti Hamzah. All rights reserved.

The author hereby grants to MIT permission to reproduce and  
distribute publicly paper and electronic copies of this thesis document  
in whole or in part.

Author .....  
Department of Mechanical Engineering  
May 22, 2012

Certified by .....  
Anette E. Hosoi  
Associate Professor of Mechanical Engineering  
MacVicar Faculty Fellow  
Thesis Supervisor

Accepted by .....  
John H. Lienhard V  
Samuel C. Collins Professor of Mechanical Engineering  
Undergraduate Officer



# The Effect of Viscoelastic Fluids on Flows Generated by Spherical Objects during Sedimentation

By

Latifah binti Hamzah

Submitted to the Department of Mechanical Engineering  
on May 22, 2012, in Partial Fulfillment of the  
Requirements for the Degree of  
Bachelor of Science in Mechanical Engineering

## Abstract

This thesis describes and analyses sedimentation experiments of a bead in various concentrations of aqueous PEG. These experiments are intended to be first order approximations of free-swimming organisms sedimenting in viscoelastic fluids and serve as a precursor to further experiments involving free-swimming organisms swimming in viscoelastic fluids. The post-processed data from these experiments are presented as colour maps in graphs of Reynolds number versus Deborah number, revealing that the velocity and vorticities are more sensitive to changes in Reynolds number than in Deborah number. However, for the range of viscoelastic fluids experimented with, no quantitative trends were apparent. As such, further experiments will need to be conducted to gain information about the velocity and viscosity maps from a wider range of viscoelastic fluids. Further improvements to the current setup are also suggested and outlined where possible.

Thesis Supervisor: Anette E. Hosoi  
Title: Associate Professor of Mechanical Engineering  
MacVicar Faculty Fellow



# Contents

<b>1</b>	<b>Introduction</b>	<b>7</b>
1.1	Central Motivations . . . . .	7
<b>2</b>	<b>Experiment Design</b>	<b>8</b>
2.1	Optical Setup . . . . .	8
2.2	Chamber Design . . . . .	8
2.2.1	Volvox Experiments . . . . .	9
2.3	Rheology . . . . .	9
<b>3</b>	<b>Experimental Procedure</b>	<b>11</b>
3.1	Preparing the Solution . . . . .	11
3.2	Sedimentation Experiments . . . . .	11
3.2.1	Chamber Modifications . . . . .	11
3.2.2	Bead Placement . . . . .	11
3.3	Object Tracking Mechanism . . . . .	12
<b>4</b>	<b>Data Analysis</b>	<b>13</b>
4.1	Preparing the Video . . . . .	13
4.2	Particle Image Velocimetry . . . . .	13
4.3	Finding Velocities . . . . .	14
4.4	Generating Colour Plots . . . . .	15
<b>5</b>	<b>Discussion</b>	<b>16</b>
5.1	Experimental Results . . . . .	16
5.2	Moving Forward . . . . .	18
<b>6</b>	<b>Future Improvements</b>	<b>19</b>
6.1	Stage Orientation . . . . .	19
6.2	PEG Chain Length and Reflection . . . . .	19
6.3	Simulating a Volvox . . . . .	20
6.4	Better Streamline Code . . . . .	20
6.5	Chamber and Experiment Design . . . . .	20
<b>7</b>	<b>Appendix - MATLAB Code</b>	<b>23</b>
7.1	Preparing Video for PIV . . . . .	23
7.2	Particle Image Velocimetry Using MATPIV Toolbox . . . . .	23

7.3	Calculating Bead Velocity . . . . .	23
7.4	Code to Make Streamline Plot as well as Colour Plots of Velocity and Vorticity . . . . .	25
<b>8</b>	<b>Bibliography</b>	<b>27</b>

## List of Figures

1	Experimental Setup . . . . .	8
2	Three Iterations of the Volvox Swimming Chamber . . . . .	9
3	Experimental Results of $G'$ versus $G''$ . . . . .	10
4	Relaxation Time Trends . . . . .	10
5	Masked Image with Coordinate System . . . . .	13
6	Velocities . . . . .	16
7	Re-De Plot for Velocities . . . . .	16
8	Vorticities . . . . .	17
9	Re-De Plot for Vorticities . . . . .	17
10	Streamlines . . . . .	17
11	Log-log Re-De Plot for Streamlines . . . . .	18

## List of Tables

1	Numbers behind Re and De Calculations . . . . .	16
---	---	----

# 1 Introduction

## 1.1 Central Motivations

Microswimmers are commonly found in viscoelastic environments; however, their behaviour in such environments remains poorly understood. Given that the potential of microswimmers operating in viscoelastic environments could achieve such lofty aims as targeted drug delivery, it is important to address some fundamental questions related to small objects translating in viscoelastic fluids. [2]

In the context of this thesis, the viscoelastic fluid in question is a solution of Standard Volvox Medium (SVM) and polyethylene glycol (PEG). The free-swimming organism ultimately intended to be used is *Volvox carteri f. nagariensis*. However, the scope of this thesis only allows for an attempt at a first order understanding of the viscoelastic problem, where the volvox has been approximated as a polystyrene bead of similar size and the viscoelastic fluid is represented by PEG dissolved in distilled water. Sedimentation experiments are thus the primary focus.

As such, the main objective of this thesis is to study the flow-field generated by the beads sedimenting in aqueous PEG in its own reference frame. This is achieved by recording their motion via a tracking microscope and performing Particle Image Velocimetry (PIV) in post-processing. The primary qualitative motivation of this study is to observe the differences between the flows generated by sedimenting beads at different concentrations of aqueous PEG in terms of the velocity and vorticity fields as well as streamlines generated. In doing so, it is hoped that there can be an identifying quantitative feature associated with these flows.

## 2 Experiment Design

### 2.1 Optical Setup

The optical experimental setup is as shown in Figure 1 and consists of a 532nm green laser, a wave plate, a beamsplitter, heat sinks, two cylindrical convex lenses, a right-angle turning mirror, and a camera mounted on a motorised stage. The main objectives here are to focus the beam as well as to transform it into a sheet that will illuminate as wide a slice of the chamber as possible.



Figure 1: Experimental Setup

### 2.2 Chamber Design

The first iterations of the chamber were undesirable because the fluid mechanics were significantly influenced by phenomena such as capillary action and wall effects. As such, the final version of the chamber was designed with dimensions of 5mm x 5mm x 60mm to minimise these effects. The main body of the chamber was machined from acrylic, with the two open sides of the chamber made of glass slides sealed using UV curable adhesive. The top was similarly made using a cover slip and also incorporates part of a pipette set at an angle, accommodating experiments conducted using volvox as it enables them to swim out of the lit beam. The chamber can then be used for multiple experiments without the data of subsequent experiments being jeopardised by the shadow cast by the volvox of preceding experiments. The main body of the chamber is machined with



two extra lips that have holes drilled through them. These are attachments points that enable the chamber to be screwed on to a platform as shown in Figure 1.

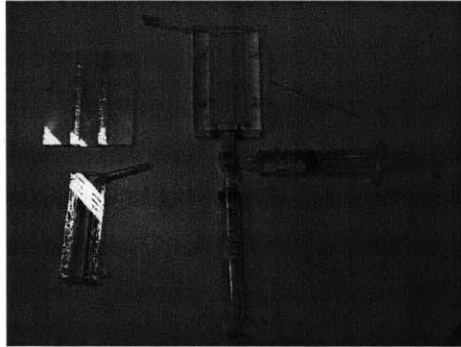


Figure 2: Three Iterations of the Volvox Swimming Chamber

### 2.2.1 Volvox Experiments

For experiments where volvox are released at the bottom of the chamber and swim or float upwards, the design of the bottom of the chamber is particularly important. It consists of a luer fitting leading to a three-way valve that connects to the main chamber as well as two syringes. The syringe perpendicular to the chamber would contain only SVM solution to allow for both the initial filling of the chamber with SVM as well as the removal of air bubbles from the three way valve. (When there are no air bubbles, the laser beam will appear as a spot at the bottom of the syringe.) The syringe parallel to the chamber contains volvox swimming in SVM. When the valve is opened between this syringe and the main chamber, the green beam of laser light encourages phototaxis and the volvox to swim up the chamber. Individual volvox are easily seen swimming through the three way valve, allowing only one volvox to be released at a time.

## 2.3 Rheology

With the idea of presenting the final result of the velocity and vorticity fields on a plot of their Reynolds number versus their Deborah number, it was necessary to measure the relaxation time of the various viscoelastic solutions used. This was done using a Small Amplitude Oscillatory Shear (SAOS) test with a linear viscoelastic strain of 0.02 and an oscillation frequency of 50Hz at a temperature of 22°C. The inverse of the frequency at which the storage modulus,  $G'$ , intersects with the loss modulus,  $G''$ , is the relaxation time. The tests were done with three concentrations of PEG solution (10%, 15% and

20%) with each test repeated three times using two samples. The results are shown in Figures 3 and 4.

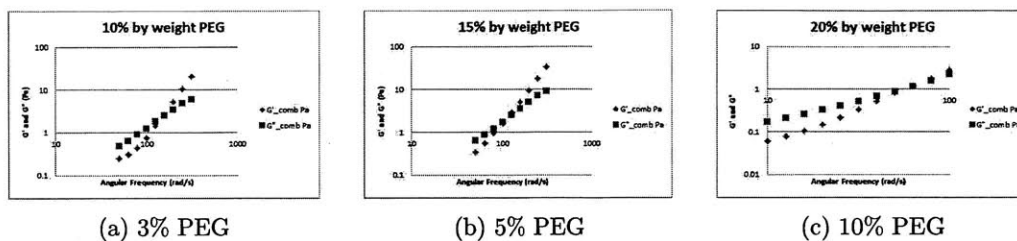


Figure 3: Experimental Results of  $G'$  versus  $G''$

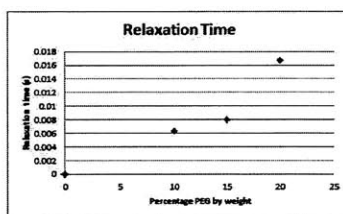


Figure 4: Relaxation Time Trends

Drawing a best fit trendline to the data presented in Figure 4 suggests that the relationship between PEG concentration and relaxation time is approximately:

$$t_r = 0.07 * conc. \quad (1)$$

Although the concentrations of the solutions used were the same, PEG 10000 was used here instead of PEG 8000 due to a shortage of PEG 8000. However, it is anticipated that such a substitution in the average chain length of the PEG molecule will result in nothing more serious than a constant multiplier factor change in the relaxation times measured. Since PEG 10000 is used consistently across all the samples, it is not expected to have a significant effect on the trends observed.

## 3 Experimental Procedure

### 3.1 Preparing the Solution

The viscoelastic fluid used was a solution of PEG 8000 in distilled water. Batches of fluid of 3%, 5%, 7.5%, 10%, 12.5% 15% and 20% PEG 8000 by mass were made by stirring the mixture with a magnetic stirrer for half an hour or until the solution looked homogeneous in a capped glass bottle to prevent evaporation. To prepare the solution for a video with the intention of PIV post-processing,  $20\mu\text{l}$  of Nile-red beads were used per 100ml of viscoelastic fluid. This type and concentration of particle was found to be optimal, allowing for good seeding without too much noise from the reflection and scatter of light due to the polymer chains.

### 3.2 Sedimentation Experiments

#### 3.2.1 Chamber Modifications

Since this thesis is primarily concerned with sedimentation experiments, in which the bead enters the chamber at the top, it was necessary to make some modifications to the chamber. Specifically, two cover slips were glued across the top with a gap between the two to allow for the insertion of the bead. The gap should be as small as possible and the fluid filled until the meniscus is as flat as possible to minimise the diffraction of the laser beam due to the curvature of the surface.

#### 3.2.2 Bead Placement

The bead was deposited on the surface of the fluid and held there by surface tension. The starting position of the camera was approximately 25mm below the surface to allow the sedimentation process to reach steady state, both in terms of reaching terminal velocity as well as for any transient effects induced by dislodging the bead from the surface. In these experiments,  $300\mu\text{m}$  Techpolymer beads from Sekisui Plastics were used. These beads were chosen as a first order approximation of a volvox from a size perspective. Although they have a greater excess density, this was found to be necessary during sedimentation experiments, especially for solutions of higher viscosity and density. It also compensates for the fact that a bead only responds to gravity, unlike Volvox, which can also respond to light stimuli.

### 3.3 Object Tracking Mechanism

The camera is mounted on a stage that allowed for movement along both the x and y axes. It is controlled by an in-house LabVIEW programme, whose primary function enables the camera to identify and centre a Volvox or other spherical object in the middle of its frame, then subsequently track it as it moves up or down the chamber. Post-processing then reveals the velocity and vorticity fields of the fluid around the bead relative to the bead's frame of reference, which allows for more data to be taken per experiment since it can track along a longer length of the chamber in more detail.

## 4 Data Analysis

Having taken videos of the sedimentation experiments, the post-processing was done in MATLAB with frequent use of the MATPIV toolbox. The ultimate objective was to be able to generate plots of Reynolds number versus Deborah number for all the experiments. The code is reproduced in the appendix.

### 4.1 Preparing the Video

Using the VideoReader and read commands, individual frames were extracted from the videos. Since this process resulted in the addition of a white border around each frame, this border was simply filled in black. It was decided not to crop the border from the image since this could result in a relative shift of the bead between frames, which in turn would affect the calculated velocity of the bead.

Once a sequence of frames had been chosen that showed good tracer density and consistent placement of the bead in the centre of each frame, one of the frames is then used to create a mask of the bead, which is excluded from the PIV analysis. This mask is saved as polymask.mat. Another frame is then used to create a world coordinate system by placing an array of dots on the black background and specifying the distance between them. The resulting file should be saved at worldco.mat. A image of a frame that has been both masked and used to generate the coordinate system is shown in Figure 5.

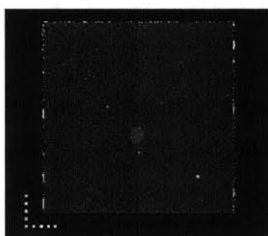


Figure 5: Masked Image with Coordinate System

### 4.2 Particle Image Velocimetry

The attached code for the PIV post-processing (published in subsection 7.1.1) analyses two adjacent frames. The main output variables of interest are  $x$ ,  $y$  and  $fuv$ . After running the code multiple times for the number of frames in the sequence, the average  $fuv$  is then taken. It is important to make sure that all the frames in each sequence have

the bead in exactly the same spot. This will ensure that there are no artificial components of velocities resulting from the camera overcompensating for any shift in the bead.

There are several parameters in the various MATPIV commands that can be adjusted for optimal results. In this case, the optimal parameters found are as follows:

- in `matpiv`: use a window shifting technique that starts with 64 x 64 images and ends with 16 x 16 images after 6 iterations with a time separation of 1/30 seconds between frames (as dictated by a combination of LabVIEW and the camera) and 50% overlap of the interrogation windows.
- in `snrfilt`: have a 1.3 threshold for the signal-to-noise ratio filter
- in `peakfilt`: have a 0.5 threshold for the peak height filter
- in `globfilt`: specify a factor of 3 as the global filter
- in `localfilt`: use a threshold of 2, a kernel size of 3 and the median method for greater robustness to outliers
- in `naninterp`: interpolate NaNs linearly [3]

### 4.3 Finding Velocities

In order to generate an Re-De plot, the velocity of the bead must be known. Given that the camera is recording everything in the frame of reference of the bead, all velocities must first be converted to the frame of reference of the lab. In this frame of reference, all velocity vectors should either be neutral or point upwards. As such, the maximum velocity from the bead's frame of reference is subtracted from all vectors.

Given that this new velocity field is now in the lab's frame of reference, the velocity of the bead is taken to be the average of all the velocity vectors adjacent to the masked out bead. Since the bead's vectors are masked and are thus NaNs, the adjacent vectors are found by running a for loop for all the NaNs vectors, specifying all eight vectors surrounding each NaN vector. Next, all double entries and all entries that were originally NaNs are set to zero and subsequently deleted. The average  $v_{fx}$  velocity of the remaining vectors is thus the velocity of the bead.

## 4.4 Generating Colour Plots

Based on the calibration of the pixels as well as the previous definition of the world coordinate map, a constant is required to change the velocity from arbitrary units into real units of m/s. In addition, recognising that the vectors contained within each frame (as opposed to in the border) were from row and column 20 to row and column 66, these were the only vectors that were plotted in the colour map.

In order for each colour map to be based on the same scale, each velocity and vorticity array had to have the same maximum and minimum values. These were determined from the experiment with the most dilute concentration of PEG. Each plot then had these maximum and minimum values artificially imposed in one corner to scale the colour map appropriately before the map was generated.

## 5 Discussion

### 5.1 Experimental Results

Based on post-processing, the calculation and values for the Reynolds and Deborah numbers are shown in Table 1 below [1]:

Table 1: Numbers behind Re and De Calculations

PEG Conc	$\rho$ (kg/m <sup>3</sup> )	$v$ (m/s)	$\mu$ (Pa*s)	Re	$t_{rel}$ (s)	$t_{exp}$ (s)	De	$V_{calc}$ (m/s)
0.03	1002	0.0324	0.0045	2.149	0.0021	0.0093	0.227	0.122
0.05	1006	0.0190	0.0054	1.057	0.0035	0.0157	0.222	0.102
0.1	1015	0.0069	0.0086	0.245	0.0063	0.0435	0.146	0.065
0.15	1023	0.0041	0.0135	0.094	0.0080	0.0731	0.109	0.041
0.2	1032	0.0011	0.0212	0.017	0.0167	0.2653	0.063	0.026

The velocity and vorticity colour plots and streamline plots are shown both individually as well as on a log-log and linear Re-De plots in figures 6 to 11. The scale across the colour maps for velocity and vorticity are the same. In general, the linear plots in particular show that Reynolds number has a dominant effect over the Deborah number since large changes in the Deborah number do not have as big an effect on the colour plots as correspondingly large changes to the Reynolds number.

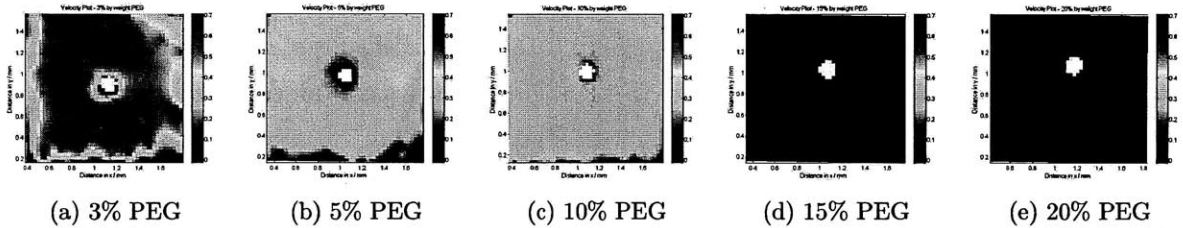


Figure 6: Velocities

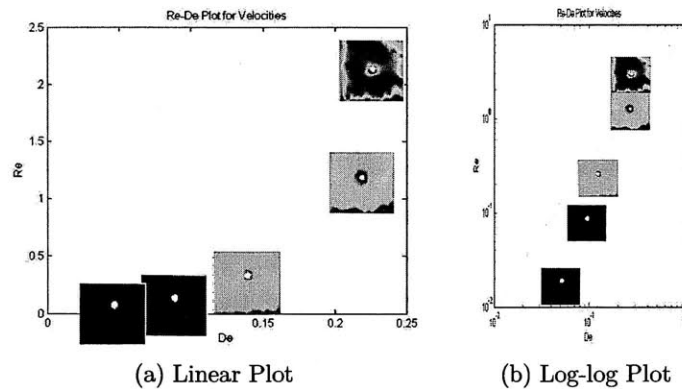


Figure 7: Re-De Plot for Velocities



The velocity maps show an increase in sedimentation velocity with a decrease in viscoelasticity, with velocity (obviously) more strongly influenced by Reynolds number than by Deborah number.

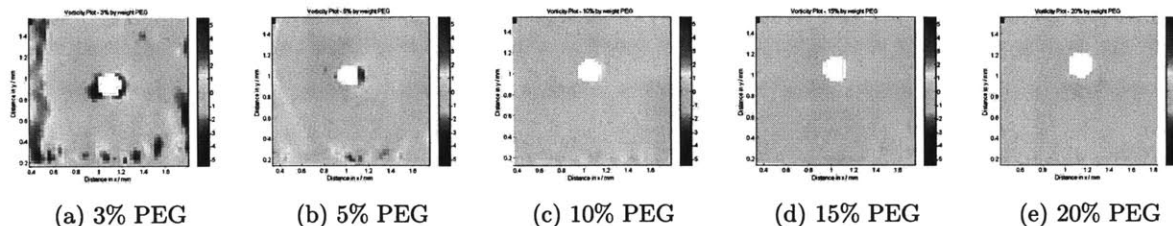


Figure 8: Vorticities

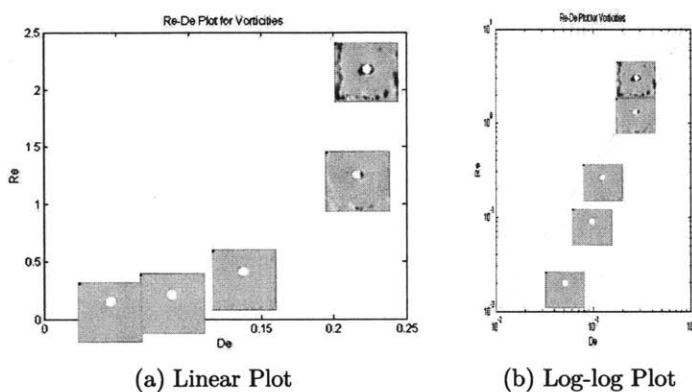


Figure 9: Re-De Plot for Vorticities

The colour maps for vorticity show more structure at higher Re and De numbers. As with the velocity, the vorticity seems to be more strongly correlated with Reynolds number than Deborah number.

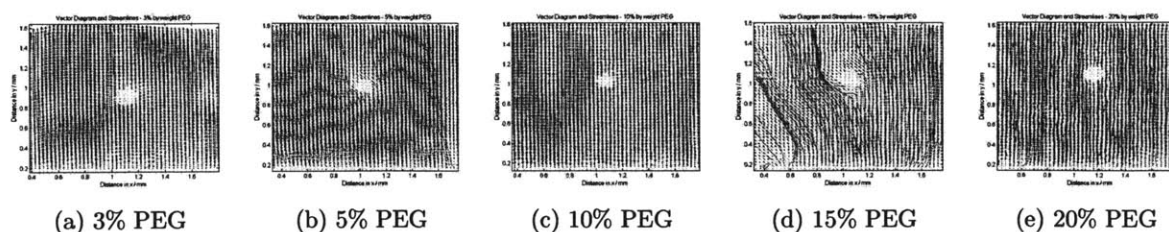


Figure 10: Streamlines

The streamlines did not seem to yield any significant trends. Having averaged the vertical velocities over 10 frames (one third of a second), the streamlines for most of the experiments seem to point straight upwards. The one anomaly was the 15% case, whose

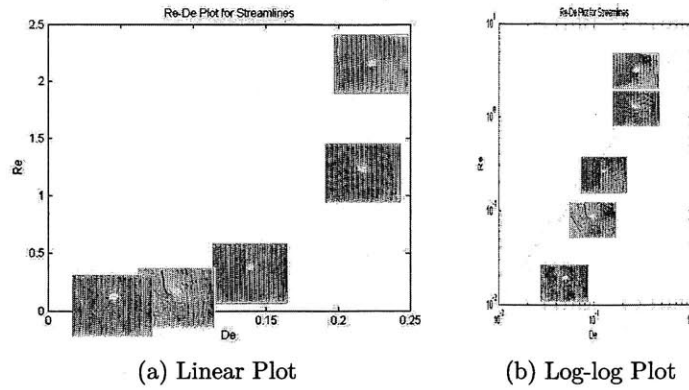


Figure 11: Log-log Re-De Plot for Streamlines

spindly, spider-like streamlines were almost undoubtedly a result of a video which seemed to be affected by unusually large amounts of circulation. Still, increasing viscosities do increase a tendency to show swirly behaviour as evidence by the increasingly less straight streamlines with increasing concentrations of PEG.

## 5.2 Moving Forward

Since there are no immediately obvious trends that emerge from the data collected thus far, the next step should be to conduct more experiments over a greater range of PEG concentrations to fill out the Re-De plots, observing if any trends emerge. In particular, it would be interesting to explore regions of higher Deborah number since small changes in De here correspond to large changes in Re and, consequently, large changes to the colour maps.

## 6 Future Improvements

### 6.1 Stage Orientation

In the current setup, the stage was oriented along a conventional x and y axis (along the horizontal and vertical). However, this was suboptimal because it tended to be difficult to capture small movements in the x direction. As a result, the stage either did not respond to small changes in x, which meant that the video captured was not exactly in the frame of reference of the bead, or it compensated too frequently with shifts that were too large, resulting in a video with jittery, monkey-like movements. This was mainly due to the fact that the motor seemed to have a minimum discrete amount that it could move.

A stage tilted at 45 degrees should be an effective solution to this problem since a small horizontal change in the location of the bead would now have component changes in both the x and y of this new stage frame, enabling small changes in the horizontal to be captured more smoothly.

### 6.2 PEG Chain Length and Reflection

Using various concentrations of aqueous PEG as the viscoelastic fluid had two main complications. Firstly, longer chains of PEG seemed to initially dissolve completely into solution but subsequently had some amount of solid precipitate out of the solution. Secondly, the PEG chains seemed to greatly scatter the laser beam, resulting in a video with less clarity and more noise. As such, the precision of the PIV post-processing was also compromised.

The easiest solution to this was to use shorter chains of PEG. For example, PEG 8000 dissolved completely into solution up to the 20% limit used in experiments. It also induced less scatter of the laser beam. However, the difference in quality between a PEG video and one of a volvox swimming in Standard Volvox Media was obvious. Perhaps the quality issues are a direct effect of the viscoelastic nature of the fluid, but perhaps even shorter PEG chains (or some other transparent viscoelastic fluid) could be used to see if there is less beam scatter. There is a tradeoff though, since shorter chain length polymers usually result in a less viscoelastic fluid.

### 6.3 Simulating a Volvox

As previously acknowledged, the plastic beads used to simulate volvox in these experiments are fairly accurate from a size perspective but not from an excess density perspective. In order to better simulate a volvox, the beads used for each experiment should have an excess density as close to that of a volvox in SVM as possible. This would require having a range of beads of different densities to account for the increasing densities of the liquid the more viscoelastic it gets.

### 6.4 Better Streamline Code

Given that the streamlines seem to be largely straight, they usually end up stopping at the interface of the bead. However, given that the tracers must continue travelling upwards by going around the bead, a better streamline code might be useful to try to complete the streamline picture. The explanation that the tracers below the bead might have gone behind the bead and into the masked region in subsequent frames is unlikely because the tracers that are in focus are usually in the same plane and rarely most significantly out of the plane. However, this effect is of course still possible for some of the tracers.

### 6.5 Chamber and Experiment Design

Although the chamber and experiment design was a significant improvement over the first iterations, convection was a still major issue. This was mainly due to capillary action and a temperature differential across the chamber. Capillary action is usually a result of improper sealing of the chamber, which can easily be remedied by ensuring that the chamber is indeed fully leak proof before any experiments are conducted. However, capillary action was also observed as a result of breaking the cover slip at the top of the chamber to deposit the bead for the sedimentation experiments.

Given that the chamber was initially designed for upward phototaxis, the chamber could probably be better designed for sedimentation experiments. Such a chamber would have to allow the bead to be deposited on the fluid in a way that does not break the surface tension without obscuring the illumination of the fluid by the laser sheet. Perhaps the exact opposite system to the phototaxis arrangement can be employed, where the chamber is lit from below and the bead is dropped in from above through a series of sealed valves.

Convection due to a temperature differential is a more difficult problem to solve, mainly because a temperature differential on the order of  $0.2^{\circ}\text{C}$  is sufficient to generate significant convection. This effect had already been reduced by employing a laser sheet, thereby heating as small an amount of the fluid as possible. Further improvements on this front would probably have to consider temperature control of the room or placing the entire chamber apparatus in a water bath of sorts.



## 7 Appendix - MATLAB Code

### 7.1 Preparing Video for PIV

```
svm9 = VideoReader('0617_SVM9.avi')
svm9_f1 = read(svm9,1); %extracts data for first frame
imshow(svm9_f1) %shows first frame

definewoco('worldco_frame.jpg','.')
mask('image.jpg', 'worldco.mat')
```

### 7.2 Particle Image Velocimetry Using MATPIV Toolbox

```
function [x,y,u,v,snr,pkh,su,sv,pu,pv,gu,gv,mu,mv,fu,fv] = gopiv(frame1,frame2,
multin,worldco,polymask,median,linear)

[x,y,u,v,snr,pkh] = matpiv(frame1, frame2,[64 64; 64 64; 32 32; 32 32; 16 16;
16 16], 1/30, 0.5, multin, worldco, polymask);
[su,sv] = snrfilt(x,y,u,v,snr,1.3);
[pu,pv] = peakfilt(x,y,su,sv,pkh,0.5);
[gu,gv] = globfilt(x,y,pu,pv,3);
[mu,mv] = localfilt(x,y,gu,gv,2,median,3,polymask);
[fu,fv] = naninterp(mu,mv,linear,polymask,x,y);
```

### 7.3 Calculating Bead Velocity

```
function [bead_velocity, ff_fvx_avg, ff_fvx_values] = better_bead_velocity(fvx_avg)

%subtracts far-field velocity
ff_fvx_avg = fvx_avg - max(max(fvx_avg));

[row, column] = find(isnan(fvx_avg));

num_isnans = length(row);
```

```

adjacent_column_vectors = zeros(8*num_isnans,1);
adjacent_row_vectors = zeros(8*num_isnans,1);

%creates matrix for all the adjacent vectors to every NaN found
for i = 1:num_isnans
    adjacent_column_vectors(8*(i-1)+1) = column(i) - 1;
    adjacent_row_vectors(8*(i-1)+1) = row(i) - 1;
    adjacent_column_vectors(8*(i-1)+2) = column(i) - 1;
    adjacent_row_vectors(8*(i-1)+2) = row(i);
    adjacent_column_vectors(8*(i-1)+3) = column(i) - 1;
    adjacent_row_vectors(8*(i-1)+3) = row(i) + 1;
    adjacent_column_vectors(8*(i-1)+4) = column(i);
    adjacent_row_vectors(8*(i-1)+4) = row(i) - 1;
    adjacent_column_vectors(8*(i-1)+5) = column(i);
    adjacent_row_vectors(8*(i-1)+5) = row(i) + 1;
    adjacent_column_vectors(8*(i-1)+6) = column(i) + 1;
    adjacent_row_vectors(8*(i-1)+6) = row(i) - 1;
    adjacent_column_vectors(8*(i-1)+7) = column(i) + 1;
    adjacent_row_vectors(8*(i-1)+7) = row(i);
    adjacent_column_vectors(8*(i-1)+8) = column(i) + 1;
    adjacent_row_vectors(8*(i-1)+8) = row(i) + 1;
end

%sets all double entries to zero
for j = 1:8*i
    current_row = adjacent_row_vectors(j);
    current_column = adjacent_column_vectors(j);
    for k = j+1:8*i
        if adjacent_row_vectors(k) == current_row &&
            adjacent_column_vectors(k) == current_column
            adjacent_row_vectors(k) = 0;
            adjacent_column_vectors(k) = 0;
        end
    end
end
end
end

```



```

%sets all original NaNs to zero
for n = 1:num_isnans
    current_row = row(n);
    current_column = column(n);
    for p = 1:j
        if adjacent_row_vectors(p) == current_row &&
            adjacent_column_vectors(p) == current_column
            adjacent_row_vectors(p) = 0;
            adjacent_column_vectors(p) = 0;
        end
    end
end

%deletes all zero (i.e. double) entries from arrays
shortened_row_vectors = adjacent_row_vectors(max(adjacent_row_vectors~=0, [], 2), :);
shortened_column_vectors = adjacent_column_vectors(max(adjacent_column_vectors
~=0, [], 2), :);

%finds fvx values for remaining vectors
ff_fvx_values = zeros(length(shortened_row_vectors), 1);
for m = 1:length(shortened_row_vectors)
    ff_fvx_values(m) = ff_fvx_avg(shortened_row_vectors(m),
        shortened_column_vectors(m));
end

bead_velocity = mean(ff_fvx_values);

```

## 7.4 Code to Make Streamline Plot as well as Colour Plots of Velocity and Vorticity

```

function [vel, vort, sline] = colourplots(xx\_avg, yx\_avg, fux\_avg, fvx\_avg)

%in arbitrary units
%velocity limits: -1 to 46}
%vorticity limits: -5.5 to 5.5}

```

```

%placed dots on thingy 20 pixels apart but said that they were 5 units apart}
%calibration is 0.00383019mm/pixel for all bead experiments
const = 4*0.00383019;

```

```

figure
vel = magnitude(xx\_avg*const,yx\_avg*const,fux\_avg*const,fvx\_avg*const);
vel(20,20) = 46*const;
vel(66,66) = -1*const;
pcolor(xx\_avg(20:66,20:66)*const,yx\_avg(20:66,20:66)*const,vel(20:66,20:66)),
shading flat, colorbar
title('Velocity Plot - 5\% by weight PEG')
xlabel('Distance in x / mm')
ylabel('Distance in y / mm')

```

```

figure
vort = vorticity(xx\_avg*const,yx\_avg*const,fux\_avg*const,fvx\_avg*const,
'circulation');
vort(20,20) = -5.5;
vort(21,20) = 5.5;
pcolor(xx\_avg(20:66,20:66)*const,yx\_avg(20:66,20:66)*const,vort(20:66,20:66)),
shading flat, colorbar
title('Vorticity Plot - 5\% by weight PEG')
xlabel('Distance in x / mm')
ylabel('Distance in y / mm')

```

```

figure
quiver(xx\_avg(20:66,20:66)*const,yx\_avg(20:66,20:66)*const,fux\_avg(20:66,20:66)
*const,fvx\_avg(20:66,20:66)*const,2), axis tight
hold on
sline = mstreamline(xx\_avg(20:66,20:66)*const,yx\_avg(20:66,20:66)*const,
fux\_avg(20:66,20:66)*const,fvx\_avg(20:66,20:66)*const);
title('Vector Diagram and Streamlines - 5\% by weight PEG')
xlabel('Distance in x / mm')
ylabel('Distance in y / mm')

```

## 8 Bibliography

- [1] Gonzalo-Tello, P., Camacho, F., Blazquez, G. "Density and Viscosity of Concentrated Aqueous Solutions of Polyethylene Glycol." *J. Chem. Eng. Data.* 39.3 (1994): 611-614. Print.
- [2] Lauga, E., Powers, T. R. "The Hydrodynamics of Swimming Microorganisms." *Rep. Prog. Phys.* 72 (2009) 096601.
- [3] Sveen, J. K. "An Introduction to MatPIV v. 1.6.1" (2004). Print.